第 49 卷 第 4 期
2022 年 4 月

湖南大学学报（自然科学版）
Journal of Hunan University (Natural Sciences)

Vol. 49 No. 4
April 2022

Open Access Article https://doi.org/10.55463/issn.1674-2974.49.4.3

Hydroxyapatite Scaffold Manufacturing under the Space Holder Method: Analysis of Physical Properties and Biocompatibility

Ade Indra[1*], Zakil Hadi[1], Jon Affi[2], Ismet Hari Mulyadi[2], Yudan Whulanza[3], Gunawarman[2]

[1] Department of Mechanical Engineering, Institut Teknologi Padang, Padang, Indonesia

[2] Department of Mechanical Engineering, Universitas Andalas, Padang, Indonesia

[3] Department of Mechanical Engineering, Universitas Indonesia, Depok, Indonesia

Abstract: The space holder method was applied to the manufacture of hydroxyapatite (HA) scaffolds by a pressureless sintering process. The aim is to develop the stages of making scaffold using the space holder method and to prove the readiness of the scaffold, especially from its physical properties and biocompatibility. The novelty of this work is the stages of processing scaffold materials in the form of slurries to produce green body scaffolds. Micron- and nano-sized HA powders were mixed in the form of slurry with polyvinyl alcohol (PVA) and ethanol. The PVA-containing HA was added with polymethyl methacrylate (PMMA) to have ratios ranging from 90:10 wt% to 65:35 wt%. The green bodies were prepared by uniaxial pressing at 200 MPa. The sintering was carried out by preheating at temperature of 700°C with a holding time of 1 h. The temperature was then increased to 1200°C with holding time of 3 h (heating rates were maintained at 5°C/min). The HA scaffolds were characterized by observing the phase, microstructures, and macrostructures; measuring the pores, testing their porosity and compressive strength. The biocompatibility properties were analyzed by testing for direct toxicity. The results indicated that the HA scaffolds made in this study met the standards since the compressive strength value was 2.23 MPa with 65.64% porosity and 126 μm to 385 μm pores size. SEM image showed the interconnection between the pores, the HA scaffolds made were non-toxic. The resulting scaffold has a great potential for further testing in living organisms.

Keywords: ceramics, hydroxyapatite, pressureless sintering, direct toxicity, high porosity.

空间支架法下的羟基磷灰石支架制造：物理性质和生物相容性分析

摘要：空间支架法应用于通过无压烧结工艺制造羟基磷灰石 (哈) 支架。目的是开发使用空间支架方法制作脚手架的阶段，并证明脚手架的准备情况，特别是从其物理特性和生物相容性来看。这项工作的新颖之处在于以浆料形式加工支架材料以生产生坯支架的阶段。微米级和纳米级哈粉末以浆料形式与聚乙烯醇 (聚乙烯醇) 和乙醇混合。将含有聚乙烯醇的哈与聚甲基丙烯酸甲酯 (聚甲基丙烯酸甲酯) 添加到具有范围为 90:10 重量百分比至 65:35 重量百分比的比例。通过在 200 兆帕的单轴压制制备生坯。烧结通过在 700°C 的温度和 1 小时的保持时间的温度下进行预热。然后将温度升高到 1200°C，保持时间为 3 小时（加热速率保持在 5 °C/分钟）。哈支架通过观察相、微观结构和宏观结构来表征；测量孔隙，测试孔隙率和抗压强度。通过测试直接毒性来分析生物相容性。结果表明，本研究制备的哈支架符合标准，抗压强度值为 2.23 兆帕，孔隙率为 65.64%，孔径为 126 微米至 385 微米。扫描电镜图像显示孔隙之间的相互连接，制成的哈支架是无毒的。由此产生的支架具有在活生物体中进一步测

Received: February 15, 2022 / Revised: March 10, 2022 / Accepted: March 13, 2022 / Published: April 30, 2022

Fund Project: Directorate of Higher Education, Research, and Technology, Ministry of Education, Culture, Research, and Technology, Indonesia (Contracts No. 027/LL10/GP-PTTJ/2021 and 163/SP2H/AMD/LT/DRPM/2020)

About the authors: Ade Indra, Zakil Hadi, Department of Mechanical Engineering, Institut Teknologi Padang, Padang, Indonesia; Jon Affi, Ismet Hari Mulyadi, Department of Mechanical Engineering, Universitas Andalas, Padang, Indonesia; Yudan Whulanza, Department of Mechanical Engineering, Universitas Indonesia, Depok, Indonesia; Gunawarman, Department of Mechanical Engineering, Universitas Andalas, Padang, Indonesia

Corresponding author Ade Indra, adeindra@itp.ac.id

试的巨大潜力。

关键词：陶瓷，羟基磷灰石，无压烧结，直接毒性，高孔隙率。

1. Introduction

A couple of studies have been developed, related to the manufacture of bone scaffolds with various biomaterials. The main breakthrough that needs to be discovered today is how to produce bone scaffolds with unique properties, namely high strength at high porosity. Bone scaffolds must be well-designed to mimic the structure and properties of the bone replaced [1, 2]. They should meet the standards: having compressive strength in the range of 2 MPa to 20 MPa [3], total porosity in the range of 60% to 90% [4], and pore size in the range of 100-400 μm [5]. Various methods have been developed to obtain these properties, such as the foaming method [6, 7], 3D printing method [8–11], space holder method [12, 13], and others. The space holder method is promising since it can control the pore size and percentage of porosity in advance when making green bodies. However, gaining excellent compressive strength is still a challenge in this method. This method, in manufacturing pores, requires a temporary material that will burn out during the sintering process and leave pores on the scaffold. In this context, polymethyl methacrylate (PMMA) is a promising biopolymer material due to its high biocompatibility properties at a relatively low price [14].

Hydroxyapatite (HA) with the chemical formula $Ca_{10}(PO_4)_6OH_2$ is a bio-ceramic material used to make bone scaffolds [31]. It is superior for making artificial bones due to its biocompatibility and bioactivity [15–18]. Its properties and structures are similar to those of human bones and teeth [19, 20]. It is also the main inorganic bone-hard tissue component, comprising 60-65% of the mineral phase in the bones of the human body [21]. In manufacturing a scaffold, many factors must be taken into account, such as the use of binders when making the green body. The addition of a binder to ceramic powder facilitates the tangential contact between particles, resulting in a green body with high strength [20]. The commonly used binding materials include polyvinyl alcohol (PVA), polyvinylpyrrolidone (PVP), and polyacrylamide (PAM) [22].

In this study, the researcher applied the space holder method to make HA scaffolds through a pressureless sintering process. During the manufacturing, they developed a mixing process to produce a homogeneous mixture. The green body was prepared by uniaxial pressing, followed by the sintering to create the sintered body. The scaffolds were then characterized for their physical and mechanical properties and biocompatibility. During the scaffold manufacturing process using the space holder method, many tools and materials are used. The potential for contamination of the scaffold with other materials may occur. Testing the biocompatibility of the resulting scaffold is one of the advantages of this study.

2. Materials

HA powders of 2.5 μm and 200 nm were taken from Sigma Aldrich, United States of America, while liquid PVA used as a binding agent was taken from Jaya Kimia, Indonesia. PMMA of 5 mm length and 2.4 mm diameter used for making pores was taken from MGM Grand, Indonesia. Refinement was performed to obtain the required PMMA grain size in the previously developed method [17]. As a diluent, ethanol was taken from Simi Indo Teknik, Indonesia. Finally, pure water used for all stages of the research, including density and porosity testing, was taken from Brataco, Indonesia.

3. Methods

3.1. Sample Preparation

An 80:20 wt% ratio was used to mix the HA powders, and then PVA and ethanol were added by 7.5 wt% and 2.5 times by HA weight, respectively. In the process, the mixture mixed the materials in a slurry form put in a drum mixer at 100 rpm (MRD – MELab.itp, drum length – 55 mm, drum diameter – 40 mm) while alumina balls were inside (3-4 mm in diameter, 30 pieces) for 2 h. To remove the ethanol, the mixture was dried at room temperature for 48 h. Afterwards, the HA chunks with PVA inside were crashed in MRD with alumina balls for 2 h. As a pore-making material, PMMA was added to the HA mixture containing PVA. The mixed ratios were 90:10, 85:15, 80:20, 75:25, 70:30, and 65:35 wt%, respectively. Each ratio was mixed in MRD without alumina balls for 2 h. Then, the green body was produced through uniaxial pressing at 200 MPa in a stainless steel mold of 8 mm diameter and 5 mm thickness. The process of sintering was preheated at 700°C for 1 hour to remove PMMA and PVA. The temperature was increased to 1200°C with a holding time of 3 h. Heating and cooling rates were maintained at 5°C/min during the sintering.

3.2. Sintered Body Characterization

X-ray diffraction (XRD), type PW3040/60-PANalytical Netherlands, was used to characterize the

HA scaffold crystalline phase. Meanwhile, Cu Kα anode (λ = 1.54060 Å, 2θ = 10–100°) at 30 mA and 4 kV was used in the X-ray diffractometer. Each step of the scanning process took 7.14 seconds. The porosity of the HA scaffolds was obtained by calculating the percentage of the volume of free space in the scaffold sample. Then, a digital microscope (DM-CMOS Controller 2MP AMCAP, China) was used to observe the shape of the porosity, by highlighting the bottom of the sample to differentiate the appearance of the pores and scaffold. ImageJ software was used to measure the pores to depict them with a histogram graph. Physically, interconnected pores were observed by scanning electron microscopy (SEM-Hitachi Horiba S-3400 N, Japan). Moreover, HA scaffold compressive strengths were tested using a universal testing machine (UTM Shimadzu, equipped with Mypin meter indicator (accuracy of 0.01 kg) and an MC-Pushton load cell). The loaded surfaces were refined with 5000 grid sandpapers before the compressive strength test. The test for compressive strength used the ASTM-C1424 standard test method for monotonic compressive strength of advanced ceramics at ambient temperature. The biocompatibility properties of the scaffolds from HA were tested for direct toxicity to compare living cells with dead cells on the third day.

4. Results and Discussion

4.1. Phase Analysis of HA Scaffold

The XRD test aimed to see the phase contained in the HA scaffolds after the sintering process. As explained in the sample preparation stage, several materials other than HA, namely PVA, ethanol, and PMMA, were added to make green bodies. All the added materials were expected to burn out during the sintering. The researchers, therefore, performed the XRD test to ensure that such an expectation had been realized. Fig. 1 shows the main peaks detected by the XRD. All of them were of HA. None of them represented PVA, ethanol, and PMMA, which were completely burned during the sintering process. These findings are confirmed by previous studies reporting that PVA burned out at a temperature of 600°C [23]. Another study said that PVA has a melting point at a temperature of 204°C. In this research, PVA and PMMA were heated and melted using a furnace, making both of them completely burned at a temperature of 700°C.

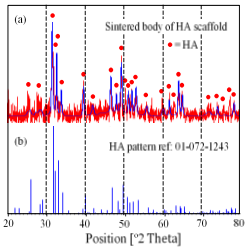

Fig. 1 XRD test: (a) HA scaffold and (b) HA reference

Table 1 presents the values of the main peaks found, compared with those of the reference HA with code 01-072-1243. The three main peaks of the HA scaffolds manufactured were at 2θ = 31.95, 33.09, and 34.28, while those of the reference HA were at 2θ = 31.74, 32.18, and 32.87. These values were very similar, indicating that the scaffolds manufactured only consisted of one phase, namely HA; while during the process of sintering, the remaining phases burned out. Thus, the scaffolds produced were quite potential as an implant material for their high biocompatibility and non-toxicity. This statement is supported by the results of the direct toxicity test (Fig. 6 and Table 2).

Table 1 The main peaks of the XRD test results on the HA scaffolds and HA reference

HA scaffold		HA pattern ref.	
°2 Theta	Intensity [%]	°2 Theta	Intensity [%]
31.95	100.00	31.74	100.00
33.09	61.93	32.18	45.30
34.28	25.77	32.87	56.40

4.2. Pores and Porosity

The pore size and the porosity percentage are the main requirements for a scaffold as a place for bone cell growth [24]. Fig. 2 shows DM images that characterize the size, shape, and distribution of the HA scaffold pores. The shapes and distributions of pores in the HA:PMMA ratios from 90:10 wt% to 65:35 wt% can be seen in Fig. 2 (a-f), showing a significant increase in the number of pores along with the increase in the amount of PMMA.

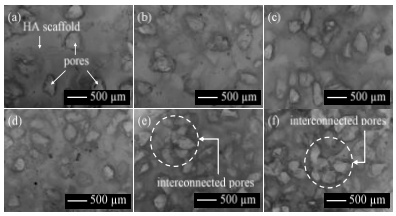

Fig. 2 DM images, HA scaffolds with varying levels of porosity: (a) 25.5%, (b) 32.9%, (c) 42.8%, (d) 49.0%, (e) 56.3%, (f) 65.6%

Fig. 3 shows a histogram graph of the results of the pore size analysis, measurement, and calculation using ImageJ software. The pore size distribution is in the range between 126 µm to 385 µm. Those with a pore size ranging from 230 µm to 307 µm reach a total of 48%, while those with a pore size ranging from 126 µm to 230 µm and from 307 µm to 385 µm reach 23% and 29%, respectively. This means that the required pore size of a scaffold, ranging from 100 µm to 400 µm, has been reached [3, 5].

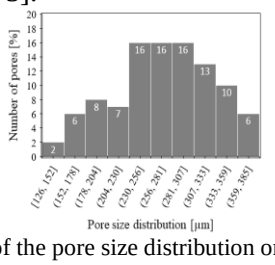

Fig. 3 Histogram of the pore size distribution on the HA scaffold

The interconnected pores of the scaffold are an absolute requirement for the growth of bone cells. Fig. 4 shows photographs and SEM images of the HA scaffold with a porosity of 65.64% that physically prove the interconnection between the pores, consistent with a previously reported study [25]. Fig. 4 (b) is an SEM image of the shape of the pores and their interconnections in the sample cut in the red field. Fig. 4 (c) is an SEM image of the pore shapes and their interconnections in the sample cut on the blue-colored planes. Both planes show the same shape and structure, proving the homogeneity of the pores on the scaffold. Fig. 4 (d) shows an SEM image that clearly shows the interconnections between the pores, so it has the potential for cell growth on the scaffold. Fig. 4 (e and f) shows SEM images showing the quite good grain bonding between micron- and nano-sized HA particles. Good and strong grains, which bond among HA particles, greatly affect the strength [20].

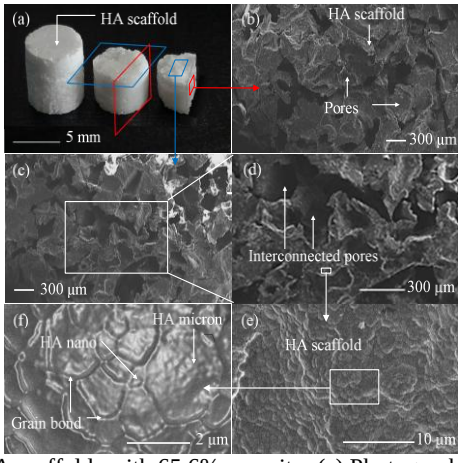

Fig. 4 HA scaffolds with 65.6% porosity: (a) Photograph of a HA scaffold sample, (b-f) SEM images of the HA scaffold microstructure

4.3. Compressive Strength

Fig. 5 shows the effect of variations in the HA:PMMA ratio on compressive strength and porosity. Adding PMMA granules will decrease the compressive strength; this is correlated with pore addition (Fig. 2). The highest compressive strength was 22.34 MPa at 90:10 wt% HA:PMMA ratio, with 25.46% porosity. The porosity increase in the HA scaffold decreased compressive strength. The 65:35 wt% ratio of HA:PMMA with a compressive strength of 2.23 MPa and 65.64% porosity fulfilled the requirements for a scaffold. Several previous studies have been conducted and reported values of porosity with compressive strength of 85% and 1.0 MPa [26], 66% and 1.6 MPa [25], 75.9% and 1.7 MPa [27], and 57% and 4.6 MPa [28], respectively. Following the standard of a scaffold, the porosity obtained in this study, namely 65.64%, has met the requirements. The porosity required for tissue growth is in the range of 60% to 90% [3, 4]. The compressive strength value in this study, namely 2.23 MPa, has passed the minimum standard, which is in the range of 1 MPa to 10 MPa [29] or in the range of 2 MPa to 12 MPa [2].

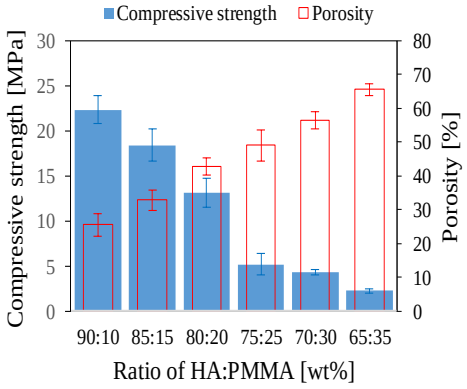

Fig. 5 The relationship between the ratio of HA:PMMA and compressive strength and porosity

4.4. Biocompatibility

The scaffolds' biocompatibility was analyzed by direct toxicity test based on the calculation of the number of live cells, by staining with trypan blue after the control cells reached 100% confluency, on the third day after seeding. 100% confluency is a condition when the cells have filled all the wells of the test site, and there is no more space for cells to multiply. The tested HA scaffolds were those that met the property requirements, namely at 65.64% porosity with 126-385 µm pores.

Based on the test results in Table 2 and Fig. 6 and 7, it can be seen that the cells experienced adhesion or sticking around the test material, indicating that the material could induce cell proliferation and was not toxic. Fig. 6 shows an analysis of the percentage of living cells compared with dead cells. In Specimen 1, there were no dead cells, meaning that 100% of the cells were alive, indicating that the HA scaffold was not toxic. In Specimen 2, 97.2% of the cells were alive in the scaffold tissue, while the remaining 2.8% were dead. In Specimen 3, 98.7% of the cells were alive in the scaffold tissue, while the remaining 1.3% were dead. A previous study reported that a scaffold is toxic if more than 50% of its cells died [30]. The three HA scaffold specimens tested had a very low percentage of dead cells, namely 1.4% on average, while 98.6% of their cells were alive. Therefore, the HA scaffolds made in this study were not toxic.

Table 2 Percentages of living and dead cells on the HA scaffold, with 65.5% porosity

Sample	Number of dead cells	Number of living cells	Total number of cells	Dead cells [%]	Living cells [%]
Control cell	0	380000	380000	0	100.0
HA scaffold-1	0	365000	365000	0	100.0
HA scaffold-2	10000	350000	360000	2.8	97.2
HA scaffold-3	5000	380000	385000	1.3	98.7
Average				1.4	98.6

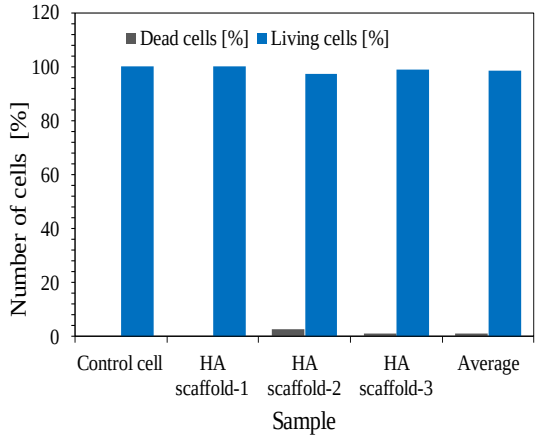

Fig. 6 Analysis of the percentages of living and dead cells

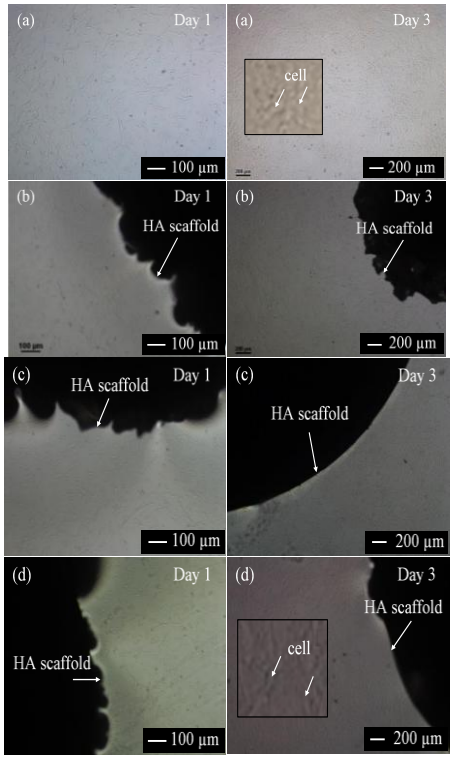

Fig. 7 Microscope images of cells in the specimens: (a) Control cell, (b-d) HA scaffold, Specimens 1, 2, and 3

5. Conclusion

The space holder method developed in this work is by controlling the stages of processing scaffold material in the form of slurry to produce green body scaffolds. The process of mixing HA with PVA added with ethanol can produce homogeneous HA slurry, so that the tangential contact between HA powder can be produced properly on the green body scaffold. Good tangential contact between HA powders can produce good grain bonds on the sintered body scaffold. The resulting HA scaffolds have met the standards of both mechanical and physical properties. It can be seen that the scaffolds showed 2.23-MPa compressive strength at 65.64% porosity, while the size of the pore ranged between 126 µm and 385 µm. The SEM images show that the pores are interconnected in the HA scaffolds. Based on the direct toxicity analysis, the HA scaffolds produced were not toxic. The XRD test results show that the scaffold comprises only the HA phase. Generally, it is known that HA is a biocompatible and non-toxic bio-ceramic. This correlates with the direct toxicity test results that the scaffold is non-toxic. A limitation of this work from a research perspective is that it has not yet reached the stage of testing on living tissues. This will be a follow-up work for future studies.

Acknowledgment

This research was funded by the Directorate of Higher Education, Research, and Technology, Ministry of Education, Culture, Research, and Technology, Indonesia, under Contracts No. 027/LL10/GP-PTTJ/2021 and 163/SP2H/AMD/LT/DRPM/2020. We would like to express our gratitude for the support and cooperation from the Ceramics Research Group of the Mechanical Engineering Study Program of Institut Teknologi Padang, the Metallurgical Laboratory of the Department of Mechanical Engineering of Universitas Andalas, and the Research Center for Biomedical Engineering of Universitas Indonesia.

References

[1] MILOVAC D., WEIGAND I., KOVAČIĆ M., IVANKOVIĆ M., and IVANKOVIĆ H. Highly porous hydroxyapatite derived from cuttlefish bone as TiO2 catalyst support. *Processing and Application of Ceramics*, 2018, 12: 136–142. https://doi.org/10.2298/pac1802136m

[2] MA H., FENG C., CHANG J., and WU C. 3D-printed bioceramic scaffolds: From bone tissue engineering to tumor therapy. *Acta Biomaterialia*, 2018, 79: 37–59. https://doi.org/10.1016/j.actbio.2018.08.026

[3] MAHAMMOD B. P., BARUA E., DEB P., DEOGHARE A. B., and PANDEY K. M. Investigation of Physico-Mechanical Behavior, Permeability and Wall Shear Stress of Porous HA/PMMA Composite Bone Scaffold. *Arabian Journal for Science and Engineering*, 2020, 45: 5505–5515. https://doi.org/10.1007/s13369-020-04467-w

[4] ROOHANI-ESFAHANI S. I., NEWMAN P., and ZREIQAT H. Design and Fabrication of 3D Printed Scaffolds with a Mechanical Strength Comparable to Cortical Bone to Repair Large Bone Defects. *Scientific Reports*, 2016, 6: 19468. https://doi.org/10.1038/srep19468

[5] SWAIN S. K. *Processing of Porous Hydroxyapatite Scaffold.* Master's thesis. Department of Ceramic Engineering, National Institute of Technology, Rourkela, 2009. http://ethesis.nitrkl.ac.in/1455/1/Binder1-sanjaya-thesis.pdf

[6] BONADIO T. G. M., FIORENTIN E. R., CANDIDO A.G., MIYAHARA R. Y., FREITAS V. F., KIYOCHI JR. H. J., HERNANDES L., ROSSO J. M., BURATO J. A., SANTOS I. A., BAESSO M. L., and WEINAND W. R. Enhanced mechanical properties and osseointegration features of CaNb2O6–PNb9O25–Ca3(PO4)2 triphasic nanostructured bioceramics derived by optimised sinterization of Nb2O5 and natural hydroxyapatite -β-tricalcium phosphate. *Ceramics International*, 2020, 46(8), Part B: 12837-12845.

https://doi.org/10.1016/j.ceramint.2020.02.054

[7] SANTOS-ROSALES V., GALLO M., JAEGER P., ALVAREZ-LORENZO C., GÓMEZ-AMOZA J. L., and GARCÍA-GONZÁLEZ C. A. New insights in the morphological characterization and modelling of poly(ε-caprolactone) bone scaffolds obtained by supercritical CO2 foaming. *Journal of Supercritical Fluids*, 2020, 166: 105012. https://doi.org/10.1016/j.supflu.2020.105012

[8] TORRES ARANGO M., ZHANG Y., ZHAO C., LI R., DOERK G., NYKYPANCHUK D., CHEN-WIEGART Y.-C. K., FLUERASU A., and WIEGART L. Ink-substrate interactions during 3D printing revealed by time-resolved coherent X-ray scattering. *Materials Today Physics*, 2020, 14: 100220. https://doi.org/10.1016/j.mtphys.2020.100220

[9] OLADAPO B. I., ZAHEDI S. A., and ADEOYE O. A. M. 3D printing of bone scaffolds with hybrid biomaterials. *Composites Part B: Engineering*, 2019, 158: 428–436. https://doi.org/10.1016/j.compositesb.2018.09.065

[10] LI K., XUE Y., YAN T., ZHANG L., and HAN Y. Si substituted hydroxyapatite nanorods on Ti for percutaneous implants. *Bioactive Materials*, 2020, 5: 116–123. https://doi.org/10.1016/j.bioactmat.2020.01.001

[11] NOSRATI H., SARRAF MAMOORY R., SVEND LE D. Q., and BÜNGER C. E. Fabrication of gelatin/hydroxyapatite/3D-graphene scaffolds by a hydrogel 3D-printing method. *Materials Chemistry and Physics*, 2020, 239: 122305. https://doi.org/10.1016/j.matchemphys.2019.122305

[12] MOTEALLEH A., EQTESADI S., PERERA F. H., ORTIZ A. L., MIRANDA P., PAJARES A., and WENDELBO R. Reinforcing bioglass scaffolds fabricated by robocasting and pressureless spark plasma sintering with graphene oxide. *Journal of the Mechanical Behavior of Biomedical Materials*, 2019, 97: 108–116. https://doi.org/10.1016/j.jmbbm.2019.05.016

[13] SAHMANI S., SHAHALI M., KHANDAN A., SABER-SAMANDARI S., and AGHDAM M. M. Analytical and experimental analyses for mechanical and biological characteristics of novel nanoclay bio-nanocomposite scaffolds fabricated via space holder technique. *Applied Clay Science*, 2018, 165: 112–123. https://doi.org/10.1016/j.clay.2018.08.013

[14] MATBOUEI A., FATHI A., RABIEE S. M., and SHIRZAD M. Layered manufacturing of a three-dimensional polymethyl methacrylate (PMMA) scaffold used for bone regeneration. *Materials Technology*, 2019, 34: 167–177. https://doi.org/10.1080/10667857.2018.1541212

[15] SHI P., LIU M., FAN F., YU C., LU W., and DU M. Characterization of natural hydroxyapatite originated from fish bone and its biocompatibility with osteoblasts. *Materials Science and Engineering: C*, 2018, 90: 706-712. https://doi.org/10.1016/j.msec.2018.04.026

[16] TURLYBEKULY A., POGREBNJAK A. D., SUKHODUB L. F., SUKHODUB L. B., KISTAUBAYEVA A. S., SAVITSKAYA I. S., SHOKATAYEVA D. H., BONDAR O. V., SHAIMARDANOV ZH. K., PLOTNIKOV S. V., SHAIMARDANOVA B. H., and DIGEL I. Synthesis, characterization, in vitro biocompatibility and antibacterial properties study of nanocomposite materials based on hydroxyapatite-biphasic ZnO micro- and nanoparticles embedded in Alginate matrix. *Materials Science and Engineering C*, 2019, 104: 109965. https://doi.org/10.1016/j.msec.2019.109965

[17] INDRA A., HADI F., MULYADI I. H., AFFI J., and GUNAWARMAN. A novel fabrication procedure for producing high strength hydroxyapatite ceramic scaffolds with high porosity. *Ceramics International*, 2021, 47: 26991–27001. https://doi.org/10.1016/j.ceramint.2021.06.112

[18] INDRA A, PUTRA A. B., HANDRA N., FAHMI H., NURZAL, ASFARIZAL, PERDANA M., ANRINAL, SUBARDI A., AFFI J., and GUNAWARMAN. Behavior of sintered body properties of hydroxyapatite ceramics: effect of uniaxial pressure on green body fabrication. *Materials Today Sustainability*, 2022, 17: 100100. https://doi.org/10.1016/j.mtsust.2021.100100

[19] TAHA M. A., YOUNESS R. A., and IBRAHIM M. Biocompatibility, physico-chemical and mechanical properties of hydroxyapatite-based silicon dioxide nanocomposites for biomedical applications. *Ceramics International*, 2020, 46: 23599–23610. https://doi.org/10.1016/j.ceramint.2020.06.132

[20] INDRA A., FIRDAUS R., MULYADI I. H., AFFI J., and GUNAWARMAN. Enhancing the physical and mechanical properties of pellet-shaped hydroxyapatite by controlling micron- and nano-sized powder ratios. *Ceramics International*, 2020, 46: 15882–15888. https://doi.org/10.1016/j.ceramint.2020.03.136

[21] VENKATESAN J., and KIM S. K. Chitosan composites for bone tissue engineering - An overview. *Marine Drugs*, 2010, 8: 2252–2266. https://doi.org/10.3390/md8082252

[22] WEI Q., WANG Y., CHAI W., ZHANG Y., and CHEN X. Molecular dynamics simulation and experimental study of the bonding properties of polymer binders in 3D powder printed hydroxyapatite bioceramic bone scaffolds. *Ceramics International*, 2017, 43: 13702–13709. https://doi.org/10.1016/j.ceramint.2017.07.082

[23] PINGAN H., MENGJUN J., YANYAN Z., and LING H. A silica/PVA adhesive hybrid material with high transparency, thermostability and mechanical strength. *RSC Advances*, 2017, 7: 2450–2459. https://doi.org/10.1039/C6RA25579E

[24] ESPOSITO CORCIONE C., GERVASO F., SCALERA F., PADMANABHAN S. K., MADAGHIELE M., MONTAGNA F., SANNINO A., LICCIULLI A., and MAFFEZZOLI A. Highly loaded hydroxyapatite microsphere/ PLA porous scaffolds obtained by fused deposition modelling. *Ceramics International*, 2019, 45: 2803–2810. https://doi.org/10.1016/j.ceramint.2018.07.297

[25] ZHANG F., LIN K., CHANG J., LU J., and NING C. Spark plasma sintering of macroporous calcium phosphate scaffolds from nanocrystalline powders. *Journal of the European Ceramic Society*, 2008, 28: 539–545. https://doi.org/10.1016/j.jeurceramsoc.2007.07.012

[26] TAKAHATA M., ITO M., MOTOMIYA M., et al. *A novel technique to generate autogenous graft bone using ultra-high porous hydroxyapatite scaffold on in vivo ilium in preparation for spinal interbody fusion*. 52nd Annual Meeting of the Orthopaedic Research Society Paper No. 1731, 2010.

[27] EILBAGI M., EMADI R., RAEISSI K., KHARAZIHA M., and VALIANI A. Mechanical and cytotoxicity evaluation of nanostructured hydroxyapatite-bredigite scaffolds for bone regeneration. *Materials Science and Engineering C*, 2016, 68: 603–612. https://doi.org/10.1016/j.msec.2016.06.030

[28] DU J., ZUO Y., LIN L., HUANG D., NIU L., WEI Y., WANG K., LIN Q., ZOU Q., and LI Y. Effect of hydroxyapatite fillers on the mechanical properties and osteogenesis capacity of bio-based polyurethane composite scaffolds. *Journal of the Mechanical Behavior of Biomedical Materials*, 2018, 88: 150–159. https://doi.org/10.1016/j.jmbbm.2018.08.028
[29] DEB P., BARUA E., DEOGHARE A. B., and DAS LALA S. Development of bone scaffold using Puntius conchonius fish scale derived hydroxyapatite: Physico-mechanical and bioactivity evaluations. *Ceramics International*, 2019, 45: 10004-10012. https://doi.org/10.1016/j.ceramint.2019.02.044
[30] KAMAL A. F., ISKANDRIATI D., DILOGO I. H., SIREGAR N. C., HUTAGALUNG E. U., SUSWORO R., YUSUF A. A., and BACHTIAR A. Biocompatibility of various hydroxyapatite scaffolds evaluated by proliferation of rat's bone marrow mesenchymal stem cells: An in vitro study. *Medical Journal of Indonesia*, 2013, 22: 202–208. https://doi.org/10.13181/mji.v22i4.600
[31] FADLI A., YENTI S. R., PRABOWO A., ALEDYA S. P., FADILA R., and SUSANTO R. The Synthesis of Hydroxyapatite Powder Using Shaker Mill Technique. *Journal of Southwest Jiaotong University*, 2021, 56(2): 22-31. https://doi.org/10.35741/issn.0258-2724.56.2.3

参考文:

[1] MILOVAC D.、WEIGAND I.、KOVAČIĆ M.、IVANKOVIĆ M. 和 IVANKOVIĆ H. 以墨鱼骨作为二氧化钛催化剂载体的高度多孔羟基磷灰石。陶瓷加工与应用, 2018, 12: 136-142. https://doi.org/10.2298/pac1802136m
[2] MA H., FENG C., CHANG J., 和 WU C. 3D 打印生物陶瓷支架：从骨组织工程到肿瘤治疗。生物材料学报，2018 年，79：37-59。https://doi.org/10.1016/j.actbio.2018.08.026
[3] MAHAMMOD B. P.、BARUA E.、DEB P.、DEOGHARE A. B. 和 PANDEY K. M. 多孔透明质酸/有机玻璃复合骨支架的物理力学行为、渗透性和壁剪应力研究。阿拉伯科学与工程杂志，2020 年，45：5505–5515。https://doi.org/10.1007/s13369-020-04467-w
[4] ROOHANI-ESFAHANI S.I.、NEWMAN P. 和 ZREIQAT H. 设计和制造具有与皮质骨相当的机械强度以修复大骨缺损的 3D 打印支架。科学报告，2016，6：19468。https://doi.org/10.1038/srep19468
[5] SWAIN S. K. 多孔羟基磷灰石支架的加工。硕士论文。国家理工学院陶瓷工程系，鲁克拉，2009。http://ethesis.nitrkl.ac.in/1455/1/Binder1-sanjaya-thesis.pdf
[6] BONADIO T. G. M., FIORENTIN E. R., CANDIDO A.G., MIYAHARA R. Y., FREITAS V. F., KIYOCHI JR. H. J.、HERNANDES L.、ROSSO J. M.、BURATO J. A.、SANTOS I. A.、BAESSO M. L. 和 WEINAND W. R. 增强的铌酸钙 2O6–PNb9O25–钙 3(采购订单 4)2 三相纳米结构生物陶瓷的机械性能和骨整合特征是通过铌 2O5 和天然羟基磷灰石的优化烧结得到的-β-磷酸三钙。国际陶瓷，2020 年，46(8)，乙部分：12837-12845。https://doi.org/10.1016/j.ceramint.2020.02.054
[7] SANTOS-ROSALES V.、GALLO M.、JAEGER P.、ALVAREZ-LORENZO C.、GÓMEZ-AMOZA J. L. 和 GARCÍA-GONZÁLEZ C. A. 聚（ε-己内酯）骨支架形态表征和建模的新见解通过超临界二氧化碳 发泡获得。超临界流体杂志，2020，166：105012. https://doi.org/10.1016/j.supflu.2020.105012
[8] TORRES ARANGO M., ZHANG Y., ZHAO C., LI R., DOERK G., NYKYPANCHUK D., CHEN-WIEGART Y.-C. K.、FLUERASU A. 和 WIEGART L. 时间分辨相干 X 射线散射揭示了 3D 打印过程中的墨水-基材相互作用。今日材料物理学，2020，14：100220. https://doi.org/10.1016/j.mtphys.2020.100220
[9] OLADAPO B. I.、ZAHEDI S. A. 和 ADEOYE O. A. M. 使用混合生物材料进行骨支架的 3D 打印。复合材料乙部分：工程，2019，158：428–436。https://doi.org/10.1016/j.compositesb.2018.09.065
[10] LI K., XUE Y., YAN T., ZHANG L., 和 HAN Y. 硅取代钛上的羟基磷灰石纳米棒用于经皮植入物。生物活性材料，2020 年，5：116–123。https://doi.org/10.1016/j.bioactmat.2020.01.001
[11] NOSRATI H.、SARRAF MAMOORY R.、SVEND LE D.Q. 和 BÜNGER C.E. 通过水凝胶 3D 打印方法制造明胶/羟基磷灰石/3D-石墨烯支架。材料化学与物理，2020，239：122305. https://doi.org/10.1016/j.matchemphys.2019.122305
[12] MOTEALLEH A., EQTESADI S., PERERA F. H., ORTIZ A. L., MIRANDA P., PAJARES A., 和 WENDELBO R. 用自动广播和无压放电等离子烧结与氧化石墨烯制造的增强生物玻璃支架。生物医学材料力学行为杂志，2019，97：108-116。https://doi.org/10.1016/j.jmbbm.2019.05.016
[13] SAHMANI S.、SHAHALI M.、KHANDAN A.、SABER-SAMANDARI S. 和 AGHDAM M. 通过空间支架技术制造的新型纳米粘土生物纳米复合材料支架的机械和生物学特性的分析和实验分析。应用粘土科学，2018，165：112-123。https://doi.org/10.1016/j.clay.2018.08.013
[14] MATBOUEI A.、FATHI A.、RABIEE S. M. 和 SHIRZAD M. 分层制造用于骨再生的三维聚甲基丙烯酸甲酯(聚甲基丙烯酸甲酯)支架。材料技术，2019 年，34：167–177。https://doi.org/10.1080/10667857.2018.1541212
[15] SHI P., LIU M., FAN F., YU C., LU W., 和 DU M. 源自鱼骨的天然羟基磷灰石的表征及其与成骨细胞的生物相容性。材料科学与工程：C，2018，90：706-712。https://doi.org/10.1016/j.msec.2018.04.026
[16] TURLYBEKULY A., POGREBNJAK A. D., SUKHODUB L. F., SUKHODUB L. B., KISTAUBAYEVA A. S., SAVITSKAYA I. S., SHOKATAYEVA D. H., BONDAR O. V., SHAIMARDANOV ZH. K.、PLOTNIKOV S. V.、SHAIMARDANOVA B. H. 和 DIGEL I. 基于嵌入海藻酸盐基质中的羟基磷灰石-双相氧化锌微米和纳米颗粒的纳米复合材料的合成、表征、体外生物相容性和抗菌性能研究。材料科学与工程 C，2019，104：109965. https://doi.org/10.1016/j.msec.2019.109965
[17] INDRA A.、HADI F.、MULYADI I.H.、AFFI J. 和 GUNAWARMAN。一种用于生产具有高孔隙率的高强度

羟基磷灰石陶瓷支架的新型制造工艺。国际陶瓷，2021 年，47：26991–27001。https://doi.org/10.1016/j.ceramint.2021.06.112

[18] INDRA A、PUTRA A. B.、HANDRA N.、FAHMI H.、NURZAL、ASFARIZAL、PERDANA M.、ANRINAL、SUBARDI A.、AFFI J. 和 GUNAWARMAN。羟基磷灰石陶瓷烧结体特性的行为：单轴压力对生坯制造的影响。今日材料可持续性，2022 年，17：100100。https://doi.org/10.1016/j.mtsust.2021.100100

[19] TAHA M. A.、YOUNESS R. A. 和 IBRAHIM M. 用于生物医学应用的羟基磷灰石基二氧化硅纳米复合材料的生物相容性、物理化学和机械性能。国际陶瓷，2020 年，46：23599–23610。https://doi.org/10.1016/j.ceramint.2020.06.132

[20] INDRA A.、FIRDAUS R.、MULYADI I.H.、AFFI J. 和 GUNAWARMAN。通过控制微米和纳米尺寸的粉末比例来提高颗粒状羟基磷灰石的物理和机械性能。国际陶瓷，2020 年，46：15882–15888。https://doi.org/10.1016/j.ceramint.2020.03.136

[21] VENKATESAN J. 和 KIM S. K. 用于骨组织工程的壳聚糖复合材料 - 概述。海洋药物，2010，8：2252–2266。https://doi.org/10.3390/md8082252

[22] WEI Q., WANG Y., CHAI W., ZHANG Y., 和 CHEN X. 聚合物粘合剂在 3D 粉末打印羟基磷灰石生物陶瓷骨支架中的粘合性能的分子动力学模拟和实验研究。国际陶瓷，2017，43：13702–13709。https://doi.org/10.1016/j.ceramint.2017.07.082

[23] PINGAN H., MENGJUN J., YANYAN Z., 和 LING H. 一种具有高透明度、热稳定性和机械强度的二氧化硅/聚乙烯醇粘合剂混合材料。RSC 进展，2017，7：2450–2459。https://doi.org/10.1039/C6RA25579E

[24] ESPOSITO CORCIONE C., GERVASO F., SCALERA F., PADMANABHAN S. K., MADAGHIELE M., MONTAGNA F., SANNINO A., LICCIULLI A., 和 MAFFEZZOLI A. 通过融合获得的高负载羟基磷灰石微球/解放军多孔支架沉积建模。国际陶瓷，2019，45：2803–2810。https://doi.org/10.1016/j.ceramint.2018.07.297

[25] ZHANG F., LIN K., CHANG J., LU J., 和 NING C. 火花等离子体烧结纳米晶粉末大孔磷酸钙支架。欧洲陶瓷学会杂志，2008 年，28：539–545。https://doi.org/10.1016/j.jeurceramsoc.2007.07.012

[26] 高畑 M.，伊藤 M.，MOTOMIYA M.，等人。一种在体内髂骨上使用超高多孔羟基磷灰石支架生成自体移植骨的新技术，为脊柱椎间融合做准备。骨科研究学会第 52 届年会论文第 1731 号，2010 年。

[27] EILBAGI M.、EMADI R.、RAEISSI K.、KHARAZIHA M., 和 VALIANI A. 用于骨再生的纳米结构羟基磷灰石-布雷数字支架的机械和细胞毒性评估。材料科学与工程 C，2016，68：603–612. https://doi.org/10.1016/j.msec.2016.06.030

[28] DU J., ZUO Y., LIN L., HUANG D., NIU L., WEI Y., WANG K., LIN Q., ZOU Q., 和 LI Y. 羟基磷灰石填料对机械性能的影响生物基聚氨酯复合支架的性能和成骨能力。生物医学材料力学行为杂志，2018，88：150-159。https://doi.org/10.1016/j.jmbbm.2018.08.028

[29] DEB P.、BARUA E.、DEOGHARE A. B. 和 DAS LALA S. 使用蓬蒂乌斯鱼鳞衍生的羟基磷灰石开发骨支架：物理机械和生物活性评估。国际陶瓷，2019，45：10004-10012。https://doi.org/10.1016/j.ceramint.2019.02.044

[30] KAMAL A. F.、ISKANDRIATI D.、DILOGO I. H.、SIREGAR N. C.、HUTAGALUNG E. U.、SUSWORO R.、YUSUF A. A. 和 BACHTIAR A. 通过大鼠骨髓间充质干细胞增殖评估的各种羟基磷灰石支架的生物相容性：一项体外研究.印度尼西亚医学杂志，2013，22：202-208。https://doi.org/10.13181/mji.v22i4.600

[31] FADLI A.、YENTI S. R.、PRABOWO A.、ALEDYA S. P.、FADILA R. 和 SUSANTO R. 使用振动磨技术合成羟基磷灰石粉末。西南交通大学学报，2021，56(2)：22-31. https://doi.org/10.35741/issn.0258-2724.56.2.3